DOI: https://doi.org/10.68732/1eaf797e4b978d13

ISBN: 978-9989-2053-6-1

A Methodology for Fall of Ground Hazard Assessment in Underground Mines

A. Tursanova & A. Adoko
School of Mining and Geosciences, Nazarbayev University, Astana, Kazakhstan
amoussou.adoko@nu.edu.kz
0000-0003-1396-7811

R. Masethe
University of KwaZulu Natal, Durban, South Africa

Abstract

In this study, the FoG index, a dimensionless indicator, is introduced to quantify the FoG hazard and its influencing factors using the Rock Engineering Systems (RES) and Artificial Neural Network (ANN) approaches. The RES is applied as a practical tool for determining complex and highly nonlinear correlations among the input parameters via an interaction matrix, while ANN is implemented to objectively assign weights to the input parameters of the FoG index. The East Sary-Oba mine, located in Kazakhstan, is used as a case study. The mine, characterized by complex geological formations including faults and shear zones, faces persistent FoG hazards that challenge existing risk mitigation strategies. A FoG database with over 150 documented FoG cases, consisting of parameters such as the rock mass parameters, the excavation geometry, the excavation support conditions, and the FoG size, was employed to construct the RES interaction matrix and to derive the FoG index. The proposed index was compared with observed FoG size and the results showed excellent agreement. It was concluded that the results of this study could be used to elaborate guidelines for FoG hazard assessment in underground mines.

Keywords

Fall of Ground, Rock engineering system, ANN, Quantitative hazard assessment

1 Introduction

Fall of Ground (FoG) is a major geotechnical hazard in underground mining and remains a significant contributor to accidents, injuries, and operational disruptions (Mark, 2021). FoG incidents occur within a wide range of conditions in the form of roof fall, rib spilling, and fallouts as a result of stress concentration or structurally controlled failure or both. Industry statistics and safety reports consistently identify ground falls as one of the leading sources of risk in underground operations, despite the recent technological advances in ground control (Małkowski & Juszyński, 2021; Adoko & Kaisa, 2023). This highlights the critical importance of FoG hazard assessment for effective ground control and mine safety management. FoG is inherently a multi-factor problem governed by the interaction of numerous parameters, including rock mass quality, excavation geometry, support systems, groundwater conditions, stress relaxation, mining-induced stress changes, and presence of

adverse geological features (Wu et al., 2018; Adoko et al., 2020; Hekmatnejad et al., 2021; Zuo et al., 2024). One of the main reasons FoG incidents remain difficult to prevent is the inherent variability in rock mass properties and geological structures surrounding underground excavations (Adoko et al., 2019). In addition, relevant geological data may not always be readily available. Therefore, quantifying FoG behaviour as the mechanical response of the surrounding rock masses due to mining is essential in ground control.

Recent developments in rock engineering have introduced system-based and data-driven methods to address this task. For example, the Rock Engineering Systems (RES) approach introduced by Hudson (1992) provides a structured device for analysing complex geotechnical problems by representing the interactions among influencing parameters through an interaction matrix (Shin et al., 2009; Zhang et al., 2024; Salmi et al., 2025). However, the assignment of parameter weights in RES often relies on expert judgment, which introduces subjectivity into the analysis (Adoko et al., 2019; Zhang et al., 2024). To address that issue,this study proposes an ANN-based RES approach to objectively determine the FoG system weightsas suggested by several studies (Li et al., 2019).

2 Methods

2.1 FoG data description

The East-Sary Oba underground mine, located in Central Kazakhstan is used as a case study. It operates room-and-pillar mining systems. The mine has experienced several significant FoG incidents in recent years. Each case includes field observations and design parameters such as the excavation dimensions, rock mass condition, support, geology, groundwater, and the FoG size. The mine is characterized by structurally complex rock mass conditions, including faults, shear zones, variable lithological contacts, and calcite-filled fracture networks (Kazakhmys Corporation LLC, 2019). Ground support systems used in the mine consist mainly of steel and polymer anchor bolts and shotcrete (Shaposhnik, 2022). The ground water conditions vary, ranging from dry to localized inflow with the maximum inflow of 3.85 L/s (Issayeva et al., 2025). The selected variables employed for the FoG hazard assessment encompass 13 parameters namely, excavation type (P1), excavation span (P2), excavation height (P3), excavation depth (P4), fault presence (P5), shear zone (P6), groundwater condition (P7), support category (P8), fracture rating (P9), uniaxial compressive strength (P10), friction angle (P11) and geological conditions (P12). The dependent parameter is FoG (P13). Fig. 1 shows the correlations between parameters.

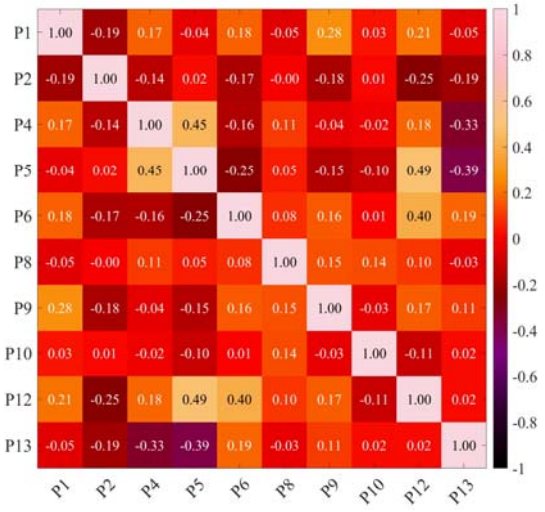


Fig. 1 Heatmap showing the correlations between the FoG and its controlling factors.

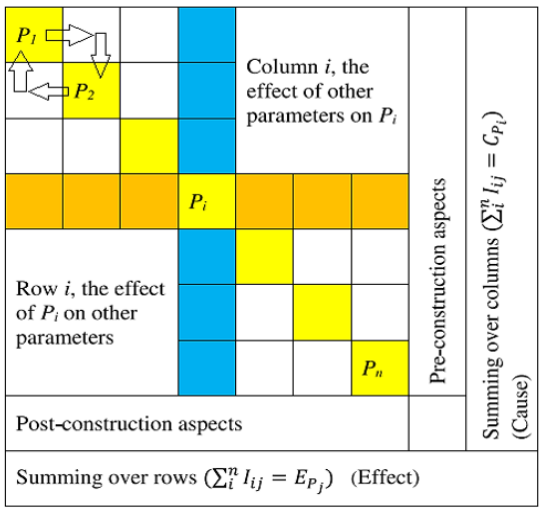


Fig.2 Illustration of the working principle of the Rock Engineering System.

2.2 Rock Engineering System (RES)

2.2.1 Basic overview of the RES

The working principle of RES is illustrated in Fig.2 and uses a cause-effect mechanism that relates every factor influencing the problem at hand (e.g. FoG) to every other factor with different weights according to their influence. An interaction matrix (IM) is constructed by positioning diagonally each

influencing parameter, P_i and P_j. Then, using a clockwise convention, their interactions are represented in the off-diagonal boxes.For a multiple-dimensional interaction matrix containing *n* input parameters P_n, a $n \times n$ matrix (i.e. n rows by n columns) is obtained. Next, the interactions (off-diagonal components $I_{ij}, (i \neq j)$) are typically rated using a semi-quantitative scale ranging from 1 to 4(Hudson, 1992), depending on the strength of the interaction. This step is known as IM encoding. The resulting ratings constitute the interaction matrix. After the matrix has been coded, the cause-effect interactions can be quantified. The sum of the row values for each parameter is called cause value and denoted as C_i, and the sum of the column values is the effect value E_i. The cause C_i, and effect E_i associated with the *ith* parameter P_i for the *ith* row and the *jth* column can be computed as (Hudson, 1992):

$$C_i = \sum_{j=1}^{n} I_{ij}; \; E_j = \sum_{i=1}^{n} I_{ij} \tag{1}$$

where I_{ij} represents the interaction components of the IM; C_i is calculated over jth column while E_j is obtained over ith row. Then, the weights assigned to each parameter influencing the FoGbehaviour can be expressed as the percentage of the sum of the system's cause and effect for such parameters according to the following equation:

$$W_i = \frac{C_i + E_i}{\sum C_i + \sum E_i} \times 100 \tag{2}$$

The FoG index describing the FoG behaviour is computed as:

$$FoG\ index = \sum W_i \times V_i \tag{3}$$

In Eq. 3 V_i denotes the rating values (Adoko et al., 2017) assigned to each the parameter P_i of FoG system. The values of FoG index can range from 0 to 100. The higher the index value, the greater the FoG risk.

2.2.2 RES weighs as the first order partial derivatives of a trained ANN

To obtain the components of the interaction matrix without using a semi-qualitative rating method, a first-order partial derivatives of a trained ANN model can be used (Li et al., 2019). The interaction components are computed using the first partial derivatives of the network output with respect to each input parameter:

$$IM_{ij} = \frac{\partial o_i}{\partial o_j} \tag{4}$$

Where o_i represents the output associated with parameter P_i, o_j represents the input corresponding to parameter P_j. These derivatives capture the sensitivity of the system response to changes in individual parameters and inherently account for nonlinear relationships learned by the ANN.

3 Results

3.1 Derivation of the RES Interaction Matrix

The FoG database described in Section 2.1 was used to train a Back Propagation Neural Network (BPNN) in order to quantify the interactions among the selected parameters. MATLAB is used for the training. The input parameters consist of the 12 selected parameters while the target variable was the FoG size. The network was configured with the *feed forward net* function. The network architecture (Fig. 3) consisted of an input layer (12 nodes), an output layer (12 nodes) and two hidden layers (10 neurons each) as suggested by recent works (Adoko et al., 2017). This configuration allows the calculation of first-order partial derivatives once the training is completed. The traditional Levenberg-Marquardt back propagation algorithm was used; the datasets were randomly divided into training, validation and testing datasets. The testing results indicated a prediction accuracy of 0.95. Fig. 4 shows the best validation performance given by the mean square error (MSE); the best validation performance was 0.00053 at epoch 37, which was considered satisfactory for this study. Table 1 presents the components of the interaction matrix after training, according to Eq. 4. As can be seen the interactions along the diagonal are almost equal to 1 highlighting an adequate training of the network.

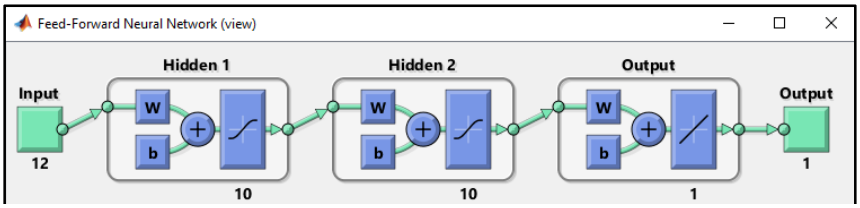


Fig. 3 ANN configuration for the FoG index.

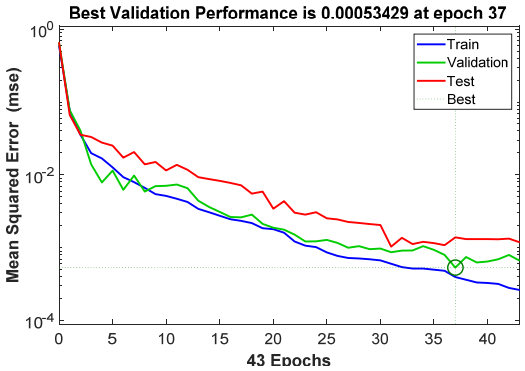


Fig. 4 Network performance.

Table 1 ANN-based interaction matrix

0.995	0.751	0.888	0.001	0.130	0.020	0.150	0.599	0.362	0.160	0.180	0.175
0.544	**0.899**	0.555	0.003	0.100	0.070	0.333	0.801	0.000	0.050	0.100	0.775
0.262	0.650	**1.001**	0.000	0.000	0.000	0.210	0.485	0.000	0.090	0.001	0.362
0.231	0.451	0.355	**0.998**	0.958	0.997	0.205	0.629	0.555	0.025	0.090	0.666
0.501	0.821	0.821	0.431	**1.000**	0.562	0.172	0.762	0.751	0.578	0.752	0.558
0.362	0.548	0.613	0.000	0.000	**1.002**	0.376	0.862	0.058	0.354	0.689	0.850
0.274	0.175	0.150	0.000	0.188	0.000	**0.998**	0.362	1.000	0.004	0.012	0.650
0.001	0.001	0.000	0.000	0.000	0.000	0.000	**1.000**	0.362	0.062	0.080	0.362
0.000	0.492	0.410	0.000	0.200	0.151	0.051	0.755	**0.971**	0.256	0.090	0.405
0.003	0.007	0.003	0.018	0.003	0.009	0.250	0.010	0.024	**1.005**	0.120	0.758
0.020	0.004	0.020	0.003	0.180	0.010	0.003	0.003	0.003	0.457	**1.001**	0.845
0.301	0.333	0.444	0.050	0.008	0.013	0.020	0.690	0.604	0.019	0.002	**1.003**

3.2 Parameter weight, intensity and dominance

The weights of the FoG system are computed according to Eqs. 1-2 and the obtained interaction matrices. The results are presented in Table 2. It can be seen that the most important parameters are P2, P5, P8 and P12 while the least important include P4, P10 and P11.

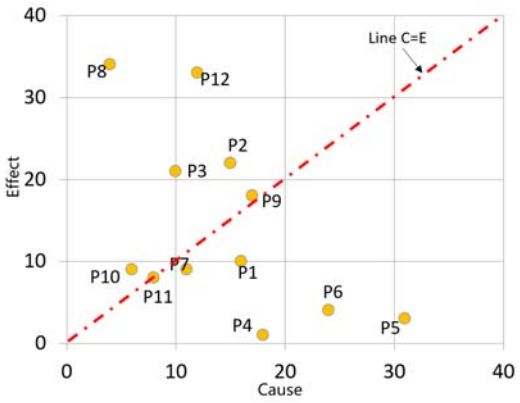


Fig. 5 Cause vs Effet plot.

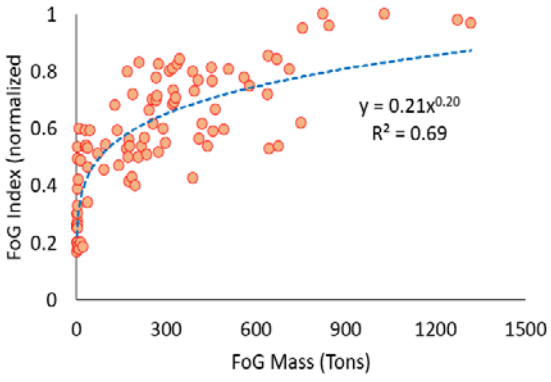


Fig. 6 Comparison between normalized FoG index and Actual Fog.

Table 2. FoG parameter weights.

	P1	**P2**	**P3**	**P4**	**P5**	**P6**	**P7**	**P8**	**P9**	**P10**	**P11**	**P12**
RES	7.6	10.8	9.0	5.5	9.9	8.1	5.8	11.0	10.2	4.4	4.7	13.1
ANN-RES	8.0	10.2	8.5	7.7	11.5	8.8	6.2	9.2	8.8	4.4	4.9	12.0

Fig.5 shows the cause-effect plot illustrating the different interactions among parameters in the FoG system. The most intense parameters include P12, P2 and P8; the most dominant parameters were P5 and P8. However, P8 influences the system more by its effect while P5 more with its cause. Meanwhile P7, P9, P10, and P11 seem to have equal cause and effect in the system. These parameters exert comparatively limited influence on FoG occurrence.

3.3 Fog index

Finally, the FoG index was calculated for the whole dataset according to Eq. 3. In order to validate the results, the FoG index values were compared with observed FoG size. The results are provided in Fig. 8. As it can be seen, a power function was used to fit the data. A coefficient of correlation of R = 0.83 (R^2 = 0.69) was obtained, indicating a strong correlation between the proposed index and the actual FoG.The index was scaled into [0,1] for convenience. Based on its definition (see Eq. 3), it integrated the 12 parameters to describe the FoG size. The FoG size can be estimated using the following empirical relationship:

$$FoG\ index_norm = 0.21 FoG^{0.20} \quad (6)$$

4 Discussions

The results indicate that fracture rating, shear zones, support category, excavation span, fault presence, and geo-engineering rating were the most influential parameters controlling the FoG Index. These findings are consistent with the dominant FoG mechanisms observed at the East Sary-Oba mine, including roof subsidence, wedge failures in shear zones, bedding-plane failures, and structurally controlled failures in faulted areas (Shaposhnik, 2022). Conversely, parameters such as intact rock UCS, friction angle, groundwater condition, excavation depth, height, and excavation type exhibited comparatively lower influence, suggesting that their influence is secondary under the geo-engineering conditions of the East Sary-Oba mine. Similar trends have been reported in recent FoG-related studies (Małkowski & Juszyński, 2021). The results further demonstrate that the integration of ANN and RES provides a robust framework for FoG hazard assessment. The ANN-based weighting process reduces the subjectivity associated with expert-driven approaches while preserving the interpretability of the RES methodology. However, the ANN architecture and hyperparameters were selected through iterative trial-and-error procedures, and the current database remains limited for broader generalization. Future studies should therefore focus on expanding the dataset, incorporating additional parameters such as blasting effect on the excavations (Imashev et al., 2024) and accounting for uncertainties in parameter properties (Adoko et al., 2011), and implementing advanced optimization techniques to improve model robustness and transferability.

5 Conclusions

This study proposed a novel FoG Index based on the integration of Rock Engineering System and ANN to quantify FoG hazards in underground excavations. Using over 100 FoG cases from the East Sary-Oba mine, the results showed that excavation span (P2), fault presence (P5), support category (P8), fracture rating (P9), and geo-engineering rating (P12) were the most influential parameters controlling FoG occurrence. Among them, P5 and P8 were identified as the dominant factors. An empirical relationship between the FoG Index and observed FoG conditions yielded a strong correlation coefficient (R= 0.83), demonstrating good agreement with field observations. The results suggest that the FoG Index can serve as apractical tool for FoG hazard assessment, ground control design, and geotechnical risk management. However, the ANN training relied on trial-and-error optimization, and the dataset remains limited for broader generalization. Future work should extend the database to additional mining sites and incorporate advanced optimization and reliability analysis techniques.

Acknowledgment

This research was funded by the Science Committee of the Ministry of Science and Higher Education of the Republic of Kazakhstan (Grant No. AP26199097). The authors also wish to acknowledge the support of Kazakhmys Company for providing an internship to the first author and for facilitating data collection at the Zhylandy Mine.

References

Adoko, A. C. & Kaisa, N. B. 2023. Development of an Expert System for Unplanned Fall of Ground Assessment in Coal Mine Excavation Intersections. In *the Proccedings of 57th U.S. Rock Mechanics/Geomechanics Symposium*. ARMA-2023-0585.

Adoko, A. C., Phumaphi, P. T. & Zvarivadza, T. 2017. Quantifying Rock Mass Behavior around Underground Excavations In *the Proccedings of The 51st US Rock Mechanics / Geomechanics Symposium, 25-28 June, San Francisco, California* ARMA.

Adoko, A. C., Vallejos, J. & Trueman, R. 2020. Stability assessment of underground mine stopes subjected to stress relaxation. *Mining Technology: Transactions of the Institute of Mining and Metallurgy*.

Adoko, A. C., Zhalel, M. & Phumaphi, P. T. 2019. Fall of ground characterization: A case study of BCL Mine, Botswana. In *the Proccedings of 53rd U.S. Rock Mechanics/Geomechanics Symposium*.

Adoko, A. C., Zuo, Q.-J. & Wu, L. 2011. A Fuzzy Model for High-Speed Railway Tunnel Convergence Prediction in Weak Rock. *Electronic Journal of Geotechnical Engineering*. 16(Q): 1275-1295.

Hekmatnejad, A., Crespin, B., Vallejos, J. A., Opazo, A. & Adoko, A. C. 2021. A hybrid predictive model of unstable rock blocks around a tunnel based on estimated volumetric fracture intensity and circular variance from borehole data sets. *Tunnelling and Underground Space Technology*. 111.

Hudson, J. A. 1992. *Rock engineering systems: theory and practice*. Chichester: Ellis Horwood.

Imashev, A., Mussin, A. & Adoko, A. C. 2024. Investigating an Enhanced Contour Blasting Technique Considering Rock Mass Structural Properties. *Applied Sciences*. 14(23): 11461.

Issayeva, L., Istekova, S., Tolybaeva, D., Togizov, K., Saurykov, Z. & Issagaliyeva, A. 2025. Petrophysical Characteristics of Geological Formations of the Zhezkazgan Ore District (Kazakhstan) and Their Relationship with Mineralization. *Minerals*. 15(11): 1106.

Kazakhmys Corporation LLC (2019). Mining plan for underground mining of the Eastern Saryoba and Western Saryoba deposits of the Zhilandy group of deposits, Head Design Institute of Kazakhmys Corporation LLC. **5.1-PZ**

Li, N., Zare Naghadehi, M. & Jimenez, R. 2019. Evaluating short-term rock burst damage in underground mines using a systems approach. *International Journal of Mining, Reclamation and Environment*: 1-31.

Małkowski, P. & Juszyński, D. 2021. Roof fall hazard assessment with the use of artificial neural network. *International Journal of Rock Mechanics and Mining Sciences*. 143: 104701.

Mark, C. 2021. An updated empirical model for ground control in U.S. multiseam coal mines. *International Journal of Mining Science and Technology*. 31(2): 163-174.

Salmi, E. F., Sellers, E. J. & Hamman, E. 2025. Rock Engineering Systems for Quantifying Risks and Controls for the Resilient Design and Optimisation of Long and Ultra-long Ore Passes. *Rock Mechanics and Rock Engineering*. 58(11): 12359-12418.

Shaposhnik, Y. N. (2022). Development of resource-saving technology for supporting mine development workings in the geomechanical conditions of the Zhilandy deposit: Intermediate stage I. Internal Expert PRO LLP report: unpublished.

Shin, H.-S., Kwon, Y.-C., Jung, Y.-S., Bae, G.-J. & Kim, Y.-G. 2009. Methodology for quantitative hazard assessment for tunnel collapses based on case histories in Korea. *International Journal of Rock Mechanics and Mining Sciences*. 46(6): 1072-1087.

Wu, L., Adoko, A. C. & Li, B. 2018. An Illustration of Determining Quantitatively the Rock Mass Quality Parameters of the Hoek–Brown Failure Criterion. *Rock Mechanics and Rock Engineering*. 51(4): 1063-1076.

Zhang, Z., Hosseini, S., Monjezi, M. & Yari, M. 2024. Extension of reliability information of Z-numbers and fuzzy cognitive map: Development of causality-weighted rock engineering system to predict and risk assessment of blast-induced rock size distribution. *International Journal of Rock Mechanics and Mining Sciences*. 178: 105779.

Zuo, Q., Li, X., Li, P., Deng, M. & Adoko, A. C. 2024. Surrounding rock instability mechanism for fault-crossing tunnels in water-rich soft rock. *Bulletin of Engineering Geology and the Environment*. 83(6).